Escola de Primavera de Transição e Turbulência
Blumenau 2020

ABCM Associação Brasileira de Engenharia e Ciências Mecânicas

12th Spring School on Transition and Turbulence
September 21st-25th, 2020, Blumenau, SC, Brazil

EPTT-2020-0007
LINEAR STABILITY ANALYSIS OF OLDROYD-B JETS

Rafael de Lima Sterza
Analice Costacurta Brandi
Universidade Estadual Paulista "Júlio de Mesquita Filho", Faculdade de Ciências e Tecnologia, Presidente Prudente
rafael.sterza@unesp.br, analice.brandi@unesp.br

Márcio Teixeira de Mendonça
Instituto de Aeronáutica e Espaço, Divisão de Propulsão Aeronáutica - CTA/IAE/APA, São José dos Campos
marciomtm@fab.mil.br

Abstract. *The study of jet flows is important in many industrial applications. In the present work, the equations that model jet flows of an Oldroyd-B type viscoelastic fluid are presented and the Linear Stability Theory (LST) is used to study the stability of the viscoelastic fluid flow to unsteady disturbances. For the LST analysis, the Orr-Sommerfeld equation is modified to include viscoelastic effects. It was observed that for high Reynolds numbers, the non-Newtonian effects do not affect the growth rates in relation to the result of the Newtonian jet, however, for low Reynolds numbers, the growth rate varies with Weissenberg number Wi and the solvent viscosity parameter β.*

Keywords: *Jet flow, Oldroyd-B fluid, Linear Stability Theory.*

1. INTRODUCTION

Fluid Mechanics is the branch of science that studies the behavior of fluids, whether the fluid is at rest or motion, it is subjected to different conditions and it behaves as per its physical properties. There are many scientific and industrial applications where the laminar flow stability and transition to turbulence are relevant and so it is important to investigate the physics of stability and laminar-turbulent transition to control, advance or prevent it (Furlan *et al.*, 2018).

One area that has made significant progress has been the area of transition to turbulence. The first investigations made by Rayleigh concerning the stability of free shear flow inviscid were investigated taking into account the viscous effects. Orr (1907) and Sommerfeld (1908) derived the equation for infinitesimal disturbance in free shear flow viscous independently (Silveria Neto, 2002). This equation takes its names today. The great difficulty in resolving it required an arduous effort to make further progress, which started to happen with Tollmien (1935) and Schlichting (1933, 1935).

Mechanisms and phenomena related to disturbances amplification in laminar flows are denoted by instability. Descriptively, instability denotes the property that the flow is subject to a change in its initial state of equilibrium if slightly disturbed. The result of a stability analysis is the growth of the initial disturbance in space (spatial instability) or in time (temporal instability) (Gaster, 1968). This growth can be measured in terms of the energy contained in the disturbance or in terms of the amplitude of the velocity fluctuations (Marxen, 2005).

The stability analysis of planar Poiseuille flow of Oldroyd-B and Giesekus fluids show that this flow becomes more unstable and the instability region of the flow is increased when β and Weissenberg (Wi) parameters are increased (Brandi *et al.*, 2017a, 2019; Furlan *et al.*, 2018). Zhang *et al.* (2013) have investigated the modal and non-modal stability of both FENE-P and Oldroyd-B fluids in channel flow. The FENE-P model includes an upper bound for the extension of polymer molecules and can more reliably represent dilute polymer solutions where significant drag reduction in the turbulent regime is observed (Zhang *et al.*, 2013). The references show that the stability of confined non-Newtonian flows have received considerable attention. On the other hand, the stability for non-Newtonian plane jet flows is little known.

The study of laminar jet flows of Newtonian fluids is of basic relevance in the mixture of polymers, extrusion, injection molding and drag reduction. It is worth mentioning that the jet flow for such fluid was studied theoretically and experimentally by Schlichting and Kestin (1968). However, polymer solutions exhibit elastic effects, in addition to non-Newtonian behavior. Thus, a complete study should include these differences (Vlachopoulos and Stournaras, 1975).

Among the first investigations, one can consider the work of Rallison and Hinch (1995), who considered the submerged elastic jet characterized by a parabolic profile flow for high Reynolds numbers. They found that the sinuous mode is fully stabilized by great elasticity, while the varicose mode is partially stabilized. In its linear stability analysis, the viscoelastic flow was modeled by the Oldroyd-B constitutive equation, and it was less unstable with the increase in the elastic effect, but not fully stable. Zhang (2012) investigated the viscoelastic jet problem, in which the Oldroyd-B model was used

for the constitutive equation. In this study, the result of the modal stability analysis in polymeric jets indicated that the elastic effect not only affected the hydrodynamic instability, increasing its critical Reynolds number, but also led to the emergence of a new instability mechanism, called elastic instability, for small numbers of Reynolds.

Thereafter, Yang *et al.* (2012, 2013) investigated the problems of electrified viscoelastic jets and viscoelastic jets surrounded by swirling air, respectively. In both studies, the linear stability analysis was considered: in the first work, a disturbance growth rate of electrified viscoelastic jets is higher than the electrified Newtonian jets for the axisymmetric mode and almost the same for the non-axisymmetric mode. In the second work, the results shown that the three-dimensional viscoelastic fluid are more unstable than Newtonian fluid flow, considering the whirlwind. More recently, Ye *et al.* (2016) investigated the axisymmetric instability of a circular jet with viscoelastic compound, in which the Oldroyd-B model was considered. Linear stability analysis was used and it was observed that the viscoelastic jet is more unstable than the Newtonian jet, regardless of whether the viscoelastic jet is totally viscoelastic or not.

In the present work the spatial linear stability analysis of two-dimensional viscoelastic jets flows for the Oldroyd-B constitutive equation are considered. Stability characteristics in terms of growth rate and phase velocity for different dimensionless non-Newtonian parameters are compared to Newtonian fluid flow results.

2. MATHEMATICAL FORMULATION

This section presents the equations that model isothermal and incompressible flows for non-Newtonian fluids. The Oldroyd-B model is considered for the extra-stress tensor.

2.1 General equations and base flow

Considering an incompressible, isothermal flow of a non-Newtonian fluid, the dimensionless governing equations are given by the continuity and momentum equations, respectively

$$\nabla \cdot \mathbf{u} = 0, \tag{1}$$

$$\frac{\partial \mathbf{u}}{\partial t} + \nabla \cdot (\mathbf{uu}) = -\nabla p + \frac{\beta}{Re}\Delta \mathbf{u} + \nabla \cdot \mathbf{T}, \tag{2}$$

where $\mathbf{u}$ denotes the velocity field, t is the time, p is the pressure, β is the dimensionless coefficient of the solvent viscosity, Re is the Reynolds number and $\mathbf{T}$ is the extra-stress tensor. Viscoelastic flows are studied in which the constitutive equation used is the Oldroyd-B model given in non-dimensional form by

$$\mathbf{T} + Wi\left[\frac{\partial \mathbf{T}}{\partial t} + \nabla \cdot (\mathbf{uT}) - \mathbf{T}(\nabla \mathbf{u})^T - (\nabla \mathbf{u})\mathbf{T}\right] = 2\frac{(1-\beta)}{Re}\mathbf{D}, \tag{3}$$

where Wi is the Weissenberg number and $\mathbf{D} = 1/2\left(\nabla \mathbf{u} + (\nabla \mathbf{u})^T\right)$ is the rate of deformation tensor.

In this paper, viscoelastic jets flows are studied. The streamwise and wall-normal directions are given by x and y, respectively and the laminar base flow is assumed parallel. The streamwise base flow velocity component is the same used by Weder (2012) and the non-Newtonian extra-stress tensor components of the base flow are given by

$$U(y) = \frac{1}{2}\left[1 + \tanh\frac{R}{4\theta}\left(\frac{R}{y} - \frac{y}{R}\right)\right], \quad T_b^{yy} = 0, \qquad T_b^{xy} = \frac{(1-\beta)}{Re}\frac{dU}{dy} \qquad \text{and} \qquad T_b^{xx} = 2WiT_b^{xy}\frac{dU}{dy}, \tag{4}$$

where R denotes the jet half-width and θ the momentum boundary layer thickness.

2.2 Linear stability theory

The Orr-Sommerfeld equation for an Oldroyd-B type viscoelastic fluid has been presented by Souza *et al.* (2016). The instantaneous flow is decomposed into two parts, a base flow and a disturbance flow. The base flow is considered parallel and invariant in the x direction. The disturbances are written as normal modes

$$\phi(x, y, t) = \overline{\phi}(y)e^{i(\alpha x - \omega t)}, \tag{5}$$

where $\overline{\phi}$ represents the magnitude and phase of the disturbances, $i = \sqrt{-1}$, $\alpha = \alpha_r + i\alpha_i$ is the wavenumber in the x direction and the spatial growth rate and ω is the angular frequency. Substituting the normal mode solution (5) into the disturbance Navier-Stokes equations and rewriting in a simplified way gives the modified Orr-Sommerfeld equation for Oldroyd-B fluid

$$\frac{d^4v}{dy^4} - \left[i(\alpha U - \omega)\frac{Re}{\beta} + 2\alpha^2\right]\frac{d^2v}{dy^2} + \left[i\frac{Re\alpha}{\beta}\frac{d^2U}{dy^2} + i\frac{Re\alpha^2}{\beta}(\alpha U - \omega) + \alpha^4\right]v +$$
$$+\frac{Re}{\beta}\left[\alpha^2\frac{dT^{xx}}{dy} - i\alpha\frac{d^2T^{xy}}{dy^2} - i\alpha^3T^{xy} - \alpha^2\frac{dT^{yy}}{dy}\right] = 0. \tag{6}$$

This equation is known as the Orr-Sommerfeld equation for a viscoelastic fluid, Oldroyd-B type (Souza *et al.*, 2016). The solution of the Orr-Sommerfeld equation corresponds to an eigenvalue problem. The solution is directly linked to the values of α, ω, Re, β and Wi, and depends on the base flow velocity profile in question (Brandi *et al.*, 2017b). The non-Newtonian extra-stress tensor components, presented in Equation (6), are given by

$$T^{yy}\left(1-i(\omega-\alpha U)Wi\right) = -Wi\left(\frac{dT_b^{yy}}{dy}v - 2i\alpha v T_b^{xy} - 2\frac{dv}{dy}T_b^{yy}\right) + \frac{2\left(1-\beta\right)}{Re}\frac{dv}{dy}, \tag{7}$$

$$T^{xy}\left(1-i(\omega-\alpha U)Wi\right) = -Wi\left(v\frac{dT_b^{xy}}{dy} - i\alpha v T_b^{xx} - \frac{dU}{dy}T^{yy} - \frac{i}{\alpha}\frac{d^2v}{dy^2}T_b^{yy}\right) + \frac{(1-\beta)}{Re}\left(i\alpha v + \frac{i}{\alpha}\frac{d^2v}{dy^2}\right), \tag{8}$$

$$T^{xx}\left(1-i(\omega-\alpha U)Wi\right) = -Wi\left(v\frac{dT_b^{xx}}{dy} + 2T_b^{xx}\frac{dv}{dy} - 2T_b^{xy}\frac{i}{\alpha}\frac{d^2v}{dy^2} - 2T^{xy}\frac{dU}{dy}\right) - \frac{2\left(1-\beta\right)}{Re}\frac{dv}{dy}. \tag{9}$$

Considering the Equations (7) – (9) together with appropriate boundary conditions one can obtain results of linear stability analysis. The Orr-Sommerfeld Equation (6) also needs to be evaluated at the boundaries for plane jet flows (Kundu and Cohen, 2010), auxiliary conditions are specified as follows

$$U_\infty = U_{\text{coflow}}, \quad \text{for} \quad y \to \pm\infty, \qquad \text{and} \qquad T_b^{xx} = T_b^{xy} = T_b^{yy} = 0.$$

In addition, all derivatives of U and T_b relative to y must be zero as $y \to \pm\infty$ and the disturbances decay exponentially away from the jet shear layer.

3. NUMERICAL RESULTS

Figure 1 shows a code verification, comparing the growth rates of non-Newtonian results with Newtonian and Rayleigh results. For this, $Re = 8400, \beta = 1$ and $Wi = 0$ were considered for both sinuous and varicose stability modes. At $Re = 8400$ viscous effects for the jet are already not relevant, showing that the stability is inviscid and due to inflexion points in the velocidty distribution. The results of the current non-Newtonian fluid implementation are in good agreement with Newtonian and Rayleigh instability results.

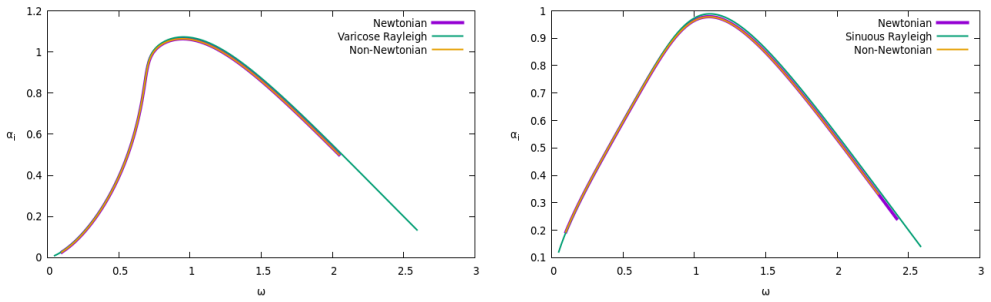

(a) Varicose mode. (b) Sinuous mode.

Figure 1. Varicose and sinuous modes growth rates variation with frequency for $Re = 8400$.

Figures 2 and 3 show the variation in the growth rate α_i with Reynolds numbers, obtained by fixing the angular frequency ω_{max} corresponding to the fastest growing mode of the Newtonian jet at $Re = 4000$.

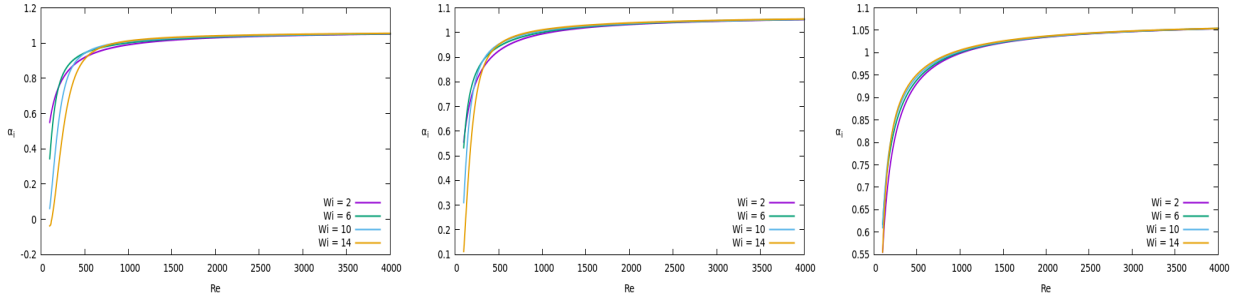

(a) (b) (c)

Figure 2. Dependency of growth rate on Reynolds number for varicose mode for (a) $\beta = 0.2$, (b) $\beta = 0.5$ and (c) $\beta = 0.8$.

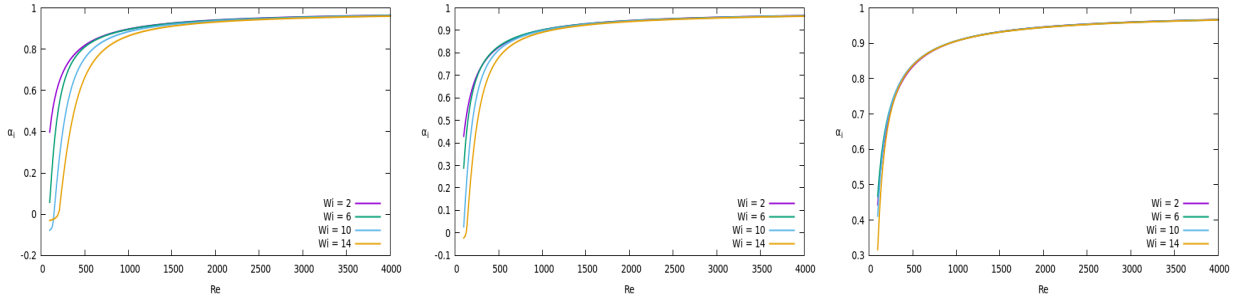

(a) (b) (c)

Figure 3. Dependency of growth rate on Reynolds number for sinuous mode for (a) $\beta = 0.2$, (b) $\beta = 0.5$ and (c) $\beta = 0.8$.

As shown in Figs. 2 and 3, as the Reynolds number increases the results become independent of the Weissenberg number and solvent viscosity parameter β. The effect of the non-Newtonian parameters become relevant at Reynolds numbers below 500, where high Weissenberg numbers and low β are the most unstable.

Table 1 shows the $\omega_{\max}$ values used to construct the graph of dependence on the growth rate on Reynolds number to varicose and sinuous modes.

Table 1. $\omega_{\max}$ angular frequency values.

	Varicose Mode			**Sinuous Mode**		
Wi	$\beta = 0.2$	$\beta = 0.5$	$\beta = 0.8$	$\beta = 0.2$	$\beta = 0.5$	$\beta = 0.8$
2	0.94043750	0.94087499	0.94174999	1.096625	1.0970625	1.0970625
6	0.93825	0.94	0.94131249	1.0975	1.0979375	1.0975
10	0.93431252	0.93781251	0.9404375	1.096625	1.0975	1.0979375
14	0.92949998	0.93562502	0.94	1.0935625	1.0970625	1.0979375

The growth rate α_i variation with angular frequency ω are presented in Figs. 4 and 5 for the varicose and sinuous modes and different Weissenberg numbers. The varicose mode highest growth rate is about 10% higher than that of the sinuous mode, but their stability characteristics are very similar, with the same range of unstable frequencies. Figure 4 shows growth rates in the varicose mode for $Re = 250$, $\beta = 0.2, 0.5$ and 0.8 and $Wi = 2, 6, 10$ and 14 and also the Newtonian fluid (considering $\beta = 1$ and $Wi = 0$).

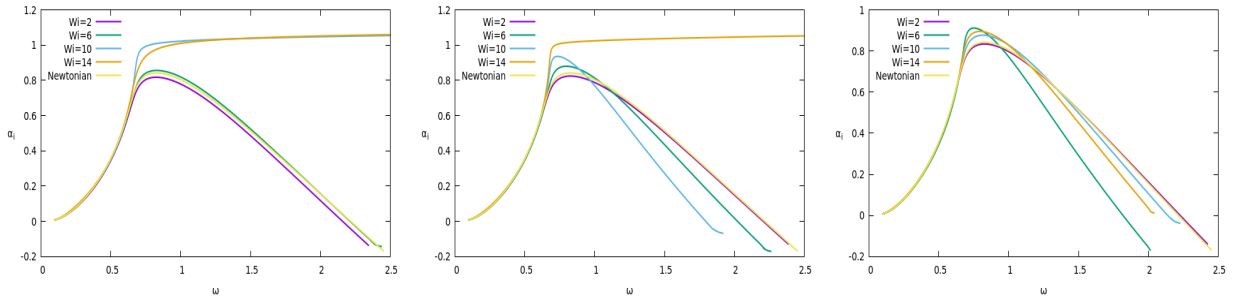

(a) (b) (c)

Figure 4. Varicose mode growth rate versus angular frequency for (a) $\beta = 0.2$, (b) $\beta = 0.5$ and (c) $\beta = 0.8$.

For the varicose mode, $\beta = 0.2$ and 0.5 and $Wi = 10$ and 14, the results are not consistent and may be spurious results, but further investigations on these modes are underway. Figure 5 shows growth rates for the sinuous mode using the same parameters as that of the varicose mode. The non-Newtonian effects are stronger for the sinuous mode, where both the maximum growth rate and range of unstable frequencies decrease with increasing Weissenberg and decreasing β parameter.

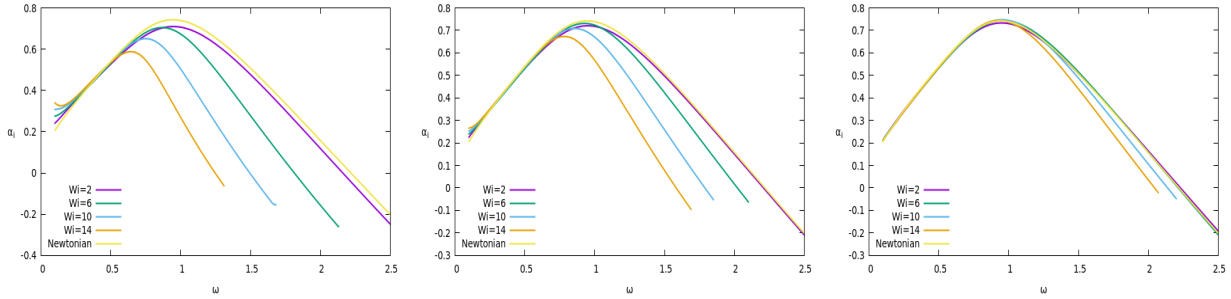

(a) (b) (c)

Figure 5. Sinuous growth rate versus angular frequency for (a) $\beta = 0.2$, (b) $\beta = 0.5$ and (c) $\beta = 0.8$.

The wavenumber α_r variation with angular frequency are presented in Figs. 6 and 7 for the varicose and sinuous modes and different Weissenberg numbers. It is worth mentioning that for $\beta = 0.2$ and 0.5 the varicose mode presented inconsistent results for some Weissenberg numbers, which are been investigated to verify if these are spurious modes or results related to elastic instability.

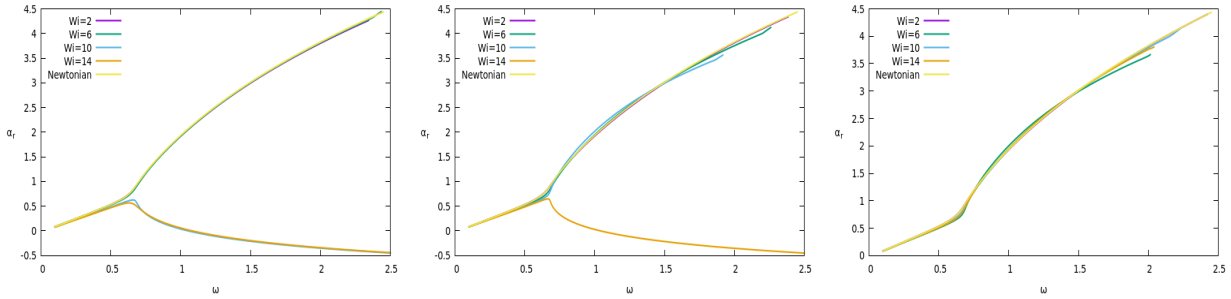

(a) (b) (c)

Figure 6. Varicose wavenumber versus angular frequency for (a) $\beta = 0.2$, (b) $\beta = 0.5$ and (c) $\beta = 0.8$.

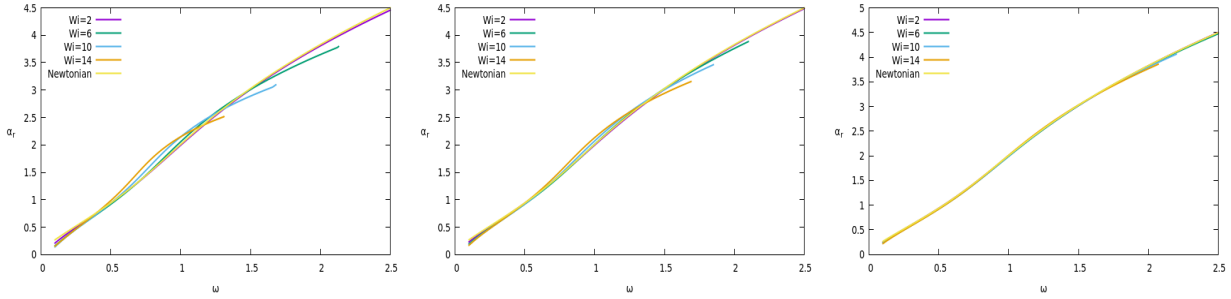

(a) (b) (c)

Figure 7. Sinuous wavenumber versus angular frequency for (a) $\beta = 0.2$, (b) $\beta = 0.5$ and (c) $\beta = 0.8$.

Figs. 8 and 9 show the variation of the disturbance phase velocity for $Re = 250$. It shows that for both the varicose and sinuous modes the disturbances are dispersive, with a strong depedence on the frequency for low frequency values. The phase velocity for the sinuous mode is more strongly dependent on non-Newtonian effects. Inconsistent results, which may be spurious mode, have been omitted.

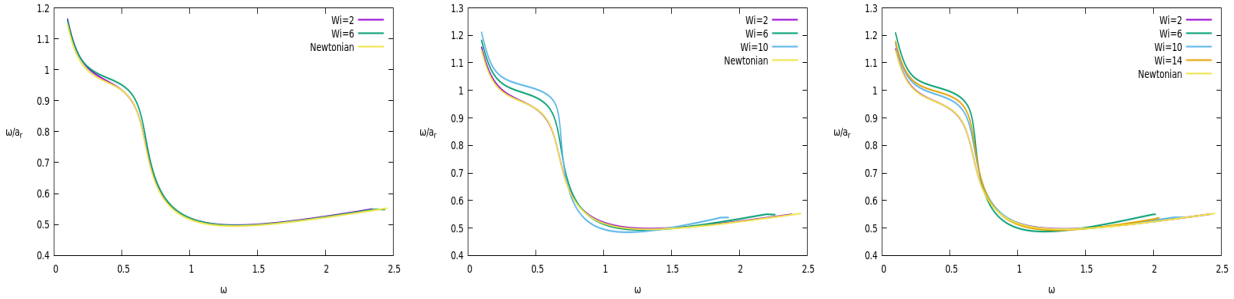

(a) (b) (c)

Figure 8. Varicose phase velocity versus angular frequency for (a) $\beta = 0.2$, (b) $\beta = 0.5$ and (c) $\beta = 0.8$.

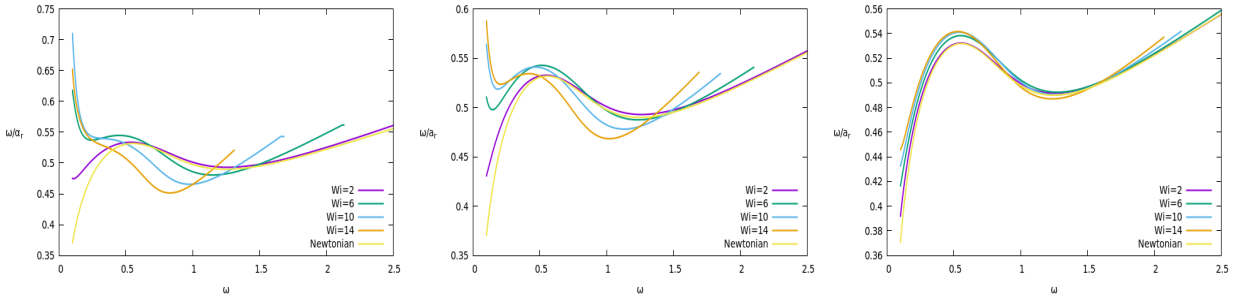

(a) (b) (c)

Figure 9. Sinuous phase velocity versus angular frequency for (a) $\beta = 0.2$, (b) $\beta = 0.5$ and (c) $\beta = 0.8$.

In order to analyze the behavior for different Reynolds values, the solvent viscosity parameter was fixed $\beta = 0.5$. The growth rate α_i variation with angular frequency ω are presented in Figs. 10 and 11 for the varicose and sinuous modes and different Reynolds and Weissenberg numbers.

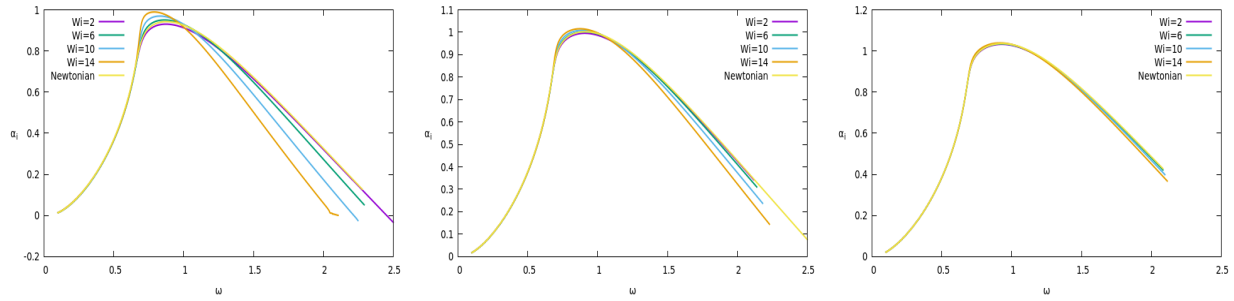

(a) (b) (c)

Figure 10. Varicose growth rates versus angular frequency for (a) $Re = 500$, (b) $Re = 1000$ and (c) $Re = 2000$.

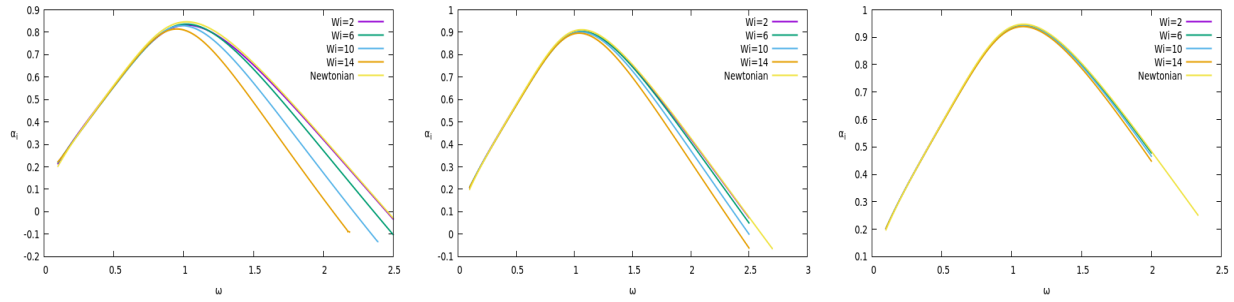

(a) (b) (c)

Figure 11. Sinuous growth rates versus angular frequency for (a) $Re = 500$, (b) $Re = 1000$ and (c) $Re = 2000$.

As the Reynolds number increases the non-Newtonian effect on the stability is reduced. Increasing further the Reynolds number results in even lower non-Newtonian effects on the results. This is expected for free-shear layers for which the stability is governed by the Rayleigh equations for high Reynolds numbers, where diffusive effects are not relevant.

Figure 12 shows the variation in the maximum growth rate with β for different Weissenberg numbers. At low values of Wi the growth rate increases with β for the varicose mode, but in general as β decreases the growth rate increases for the varicose mode and decreases for the sinuous mode. For high Wi and low β values the inconsistent results are presented as growth rates independent of β for the varicose mode.

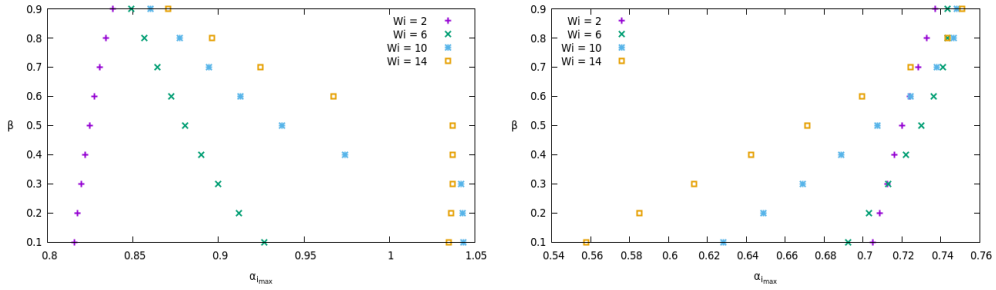

(a) Varicose mode. (b) Sinuous mode.

Figure 12. Maximum growth rate variation with β for different Weissenberg numbers for $Re = 250$.

Figure 13 shows the variation in the maximum growth rate with the Weissenberg number for different β values. For the sinuous mode, the growth rate initially increase with increaseing Wi, but above a certain value it starts to decrease. This behavior has already been observed for the stability of non-Newtonian Poiseuille flow (Brandi *et al.*, 2019).

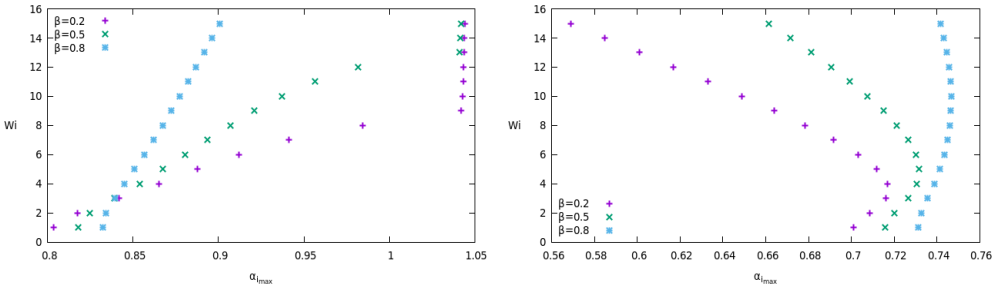

(a) Varicose mode. (b) Sinuous mode.

Figure 13. Maximum growth rate variation with the Weissenberg number for different β for $Re = 250$.

4. CONCLUSIONS

In this work, a spatial stability analysis was performed through the Linear Stability Theory for viscoelastic jet flows. The Oldroyd-B model was used and different values of dimensionless parameters were tested for non-Newtonian fluid flows. The LST code was based on a Shooting method and considered spatial disturbances for stability analysis. The LST code was verified by comparison with results obtained using the Rayleigh equation.

The results show that non-Newtonian effects are relevant at low values of Reynolds number. It was observed that as the amount of the polymer concentration in the fluid and Weissenberg number are decreased and the Reynolds number is increased the non-Newtonian effect on the stability is reduced. Furthermore, non-Newtonian effects reduce the growth rates and change the phase velocity when compared to Newtonian flows.

5. ACKNOWLEDGEMENTS

The authors thank the *Coordenação de Aperfeiçoamento de Pessoal de Nível Superior* (CAPES) for the research grant received during the development of this study.

6. REFERENCES

Brandi, A.C., Gervazoni, E.S., Mendonça, M.T. and Souza, L.F., 2017a. "Investigação da estabilidade em escoamento bidimensional para o fluido Oldroyd-B". In *Proceeding Series of the Brazilian Society of Computational and Applied*

Mathematics. São José dos Campos, Brasil.

Brandi, A.C., Mendonça, M.T. and Souza, L.F., 2017b. "Comparação de DNS e LST para o escoamento de Poiseuille do fluido Oldroyd-B". In *13º Congresso Ibero-americano de Engenharia Mecânica*. Lisboa, Portugal.

Brandi, A.C., Mendonça, M.T. and Souza, L.F., 2019. "DNS and LST stability analysis of Oldroyd-B fluid in a flow between two parallel plates". *Journal of Non-Newtonian Fluid Mechanics*, Vol. 267, pp. 14 – 27. ISSN 0377-0257.

Furlan, L.J., Brandi, A.C., Mendonça, M.T., Silva, A.A. and Souza, M.T.A.L.F., 2018. "Lst of oldroyd-b and giesekus fluids flow stability". In *ABCM Spring School on Transition and Turbulence - EPTT*. ABCM.

Gaster, M., 1968. "Growth of disturbances in both space and time". *Physics of Fluids*, Vol. 11, No. 4, pp. 723–727.

Kundu, P.K. and Cohen, I.M., 2010. *Fluid Mechanics*. Academic Press, Kidlington, 4th edition.

Marxen, O., 2005. *Numerical studies of physical effects related to the controlled transition process in laminar separation bubbles*. Ph.D. thesis, Institut für Aerodynamik und Gasdynamik der Universität Stuttgart.

Orr, W.M.F., 1907. "The stability or instability of the steady motions of a perfect liquid and of a viscous liquid. part i: A perfect liquid". *Proceedings of the Royal Irish Academy. Section A: Mathematical and Physical Sciences*, Vol. 27, pp. 9–68.

Rallison, J.M. and Hinch, E.J., 1995. "Instability of a high-speed submerged elastic jet". *J. Fluid Mech*, pp. 311–324.

Schlichting, H., 1933. "Zur enststehung der turbulenz bei der plattenstronmung". *Nachr. Ges. Wiss. Gottingen, Math-phys. K.*, Vol. 1, pp. 181–208.

Schlichting, H., 1935. "Amplitudenverteilung und energiebilanz der kleinen storungen bei der plattengrensschicht". *Nachr. Ges. Wiss. Gottingen, Math-phys. K.*, Vol. 1, pp. 14–78.

Schlichting, H. and Kestin, J., 1968. *Boundary-layer Theory*. McGraw-Hill series in mechanical engineering. McGraw-Hill.

Silveria Neto, A., 2002. *Fundamentos da Turbulência nos Fluidos*. Universidade Federal de Uberlândia.

Sommerfeld, A., 1908. "Ein beitrag zur hydrodynamischen erklarun der turbulenten flussigkeitsbewegung". *Proceedings of the fourth international congress on mathematicians*, Vol. 3, pp. 116–124.

Souza, L.F., Brandi, A.C. and Mendonça, M.T., 2016. "Estabilidade de escoamentos de fluidos não-Newtonianos". In *Turbulência*, ABCM, São José dos Campos, Brasil, Vol. 10.

Tollmien, W., 1935. "Ein allgemeines kriterium der instabilitat laminarer geschwindigkeitsverteilungen". *Nachr. Ges. Wiss. Gottingen, Math-phys. K.*, Vol. 50, pp. 79–114.

Vlachopoulos, J. and Stournaras, C., 1975. "Laminar two-dimensional non-newtonian jets". *AIChE Journal*, Vol. **21**, No. 2, pp. 385–388.

Weder, M., 2012. *Linear Stability and Acoustics of a Subsonic Plane Jet Flow*. Master's thesis, Institute of Fluid Dynamics, ETH Zurich.

Yang, L.J., Liu, Y.X. and Fu, Q.F., 2012. "Linear stability analysis of an electrified viscoelastic liquid jet". *Journal of Fluids Engineering*, Vol. 134, pp. 1–13.

Yang, L.J., Tong, M.X. and Fu, Q.F., 2013. "Linear stability analysis of a threedimensional viscoelastic liquid jet surrounded by a swirling air stream". *Journal of Non-Newtonian Fluid Mechanics*, Vol. 191, pp. 1–13.

Ye, H.Y., Yang, L.J. and Fu, Q.F., 2016. "Instability of viscoelastic compound jets". *Physics of Fluids*, Vol. 28, p. 043101.

Zhang, M., 2012. *Linear stability analysis of viscoelastic flows*. Master's thesis, Royal Institute of Technology.

Zhang, M., Lashgari, I., Zaki, T.A. and Brandt, L., 2013. "Linear stability analysis of channel flow of viscoelastic Oldroyd-B and FENE-P fluids". *Journal of Fluid Mechanics*, Vol. 737, pp. 249 – 279.

7. RESPONSIBILITY NOTICE

The authors are the only responsible for the printed material included in this paper.